Kethoxal Inactivation of Three Transfer Ribonucleic Acids Chargeable by Yeast Phenylalanyl Transfer Ribonucleic Acid Synthetase†

Michael Litt* and Carol M. Greenspan‡

ABSTRACT: Several tRNA species can be aminoacylated by yeast phenylalanyl-tRNA synthetase. We have studied the reaction of kethoxal with three of these tRNAs: yeast $tRNA^{Phe}$, *Escherichia coli* $tRNA^{Phe}$, and *Escherichia coli* $tRNA_1^{Val}$. When guanine is present at positions 20 or 34 in these molecules, it reacts readily with kethoxal with concomitant partial loss of phenylalanine acceptor activity. The ability of *Escherichia coli* $tRNA_1^{Val}$ to be aminoacylated by *Escherichia coli* valyl-tRNA synthetase is unimpaired by kethoxalation. Inactivation of yeast $tRNA^{Phe}$ by kethoxal is a single-hit process. Combined with our previous studies on this tRNA, these results suggest that either site 20 or 34 can act as a target for inactivation, if the bulky α-ethoxyethyl side chain of the kethoxal moiety is properly oriented.

For several years, we have been using kethoxal as a probe for guanines in single-stranded regions of tRNAs. We showed that guanine sites 20 and 34 in yeast $tRNA^{Phe}$ can be specifically modified with resulting partial loss of phenylalanine acceptance (Litt, 1969). Further studies on the modification of this tRNA with kethoxal and glyoxal suggested that the presence of a bulky substituent on the glyoxal moiety and the proper stereochemical orientation of this substituent were essential for inactivation (Litt, 1971).

However, these studies did not allow us to decide which of the two sites was the target for inactivation. Indeed, we could not exclude the possibilities that either site could serve as a target or that inactivation was a two-hit process requiring kethoxalation of both sites. In this report, we show that inactivation of (yeast) $tRNA^{Phe}$ by kethoxal is a single-hit process.

Escherichi coli $tRNA_1^{Val}$ and *Escherichia coli* $tRNA^{Phe}$ can be charged with phenylalanine by (yeast) Phe-tRNA synthetase[1] and hence must have a recognition site for this enzyme. On the basis of sequence analogies, Dudock *et al.* (1971) have proposed that this recognition site is contained in the stem of the dihydrouridine loop. As G-20 in yeast $tRNA^{Phe}$ is located adjacent to this putative recognition site, we proposed that it was probably the target for inactivation (Litt, 1971). Since *E. coli* $tRNA_1^{Val}$ also has a G at position 20 (but not at 34), we predicted that its ability to be charged with phenylalanine by yeast Phe-tRNA synthetase would also be inactivated by kethoxalation at that site. Conversely, if G-34 were not a target for inactivation, kethoxalation of (*E. coli*) $tRNA^{Phe}$ (which lacks a G at position 20 but has one at position 34) should not inactivate the charging of this molecule by yeast Phe-tRNA synthetase. In this report we present the results of experiments designed to test these predictions.

Methods

tRNA. Yeast $tRNA^{Phe}$ was prepared by the method of Litt (1968) and accepted 1400 pmoles of phenylalanine/A_{260} unit. (*E. coli*) $tRNA_1^{Val}$ and $tRNA^{Phe}$ were prepared by several steps of BD-cellulose chromatography starting with commercial tRNA from *E. coli* B (Schwarz/Mann). The first chromatography step was essentially the same as described in the legend to Figure 1 of Dudock *et al.* (1970). The $tRNA_1^{Val}$ appeared early in the salt gradient, whereas $tRNA^{Phe}$ and $tRNA^{Trp}$ were eluted in the "ethanol fraction" obtained by washing the column with 1 M NaCl–0.010 M $MgCl_2$ in 9.5% (w/v) ethanol after completion of the salt gradient.

Further purification of (*E. coli*) $tRNA_1^{Val}$ and $tRNA^{Phe}$ was accomplished by BD-cellulose chromatography of the phenoxyacetylaminoacyl-tRNAs, using solutions A–F as described by Gillam *et al.* (1968). $tRNA_1^{Val}$ isolated in this way accepted 1100 pmoles of valine per A_{260} unit.

The ethanol fraction from the first BD-cellulose column contained $tRNA^{Trp}$ as well as $tRNA^{Phe}$. These two tRNAs were purified by two successive cycles of aminoacylation, phenoxyacetylation, and BD-cellulose chromatography. $tRNA^{Phe}$ so obtained was used in these studies; experiments utilizing the $tRNA^{Trp}$ will be reported elsewhere. In the first cycle, the tRNA (1000 A_{260} units) was charged with tryptophan, phenoxyacetylated, and chromatographed on a 0.9 × 20 cm BD-cellulose column. The column was eluted successively with solution B, solution E, and a linear gradient (25 ml each) using solution E as starting buffer and solution F as limit buffer. $tRNA^{Phe}$ eluted with solution E whereas phenoxyacetyltryptophanyl-$tRNA^{Trp}$ eluted with the gradient. In the second cycle, $tRNA^{Phe}$ obtained from the first cycle was charged with [^{14}C]phenylalanine, phenoxyacetylated, and rechromatographed on the 0.9 × 20 cm BD-cellulose column under conditions identical with those used for the first cycle. The phenoxyacetylphenylalanyl-$tRNA^{Phe}$, which emerged with the gradient, had a phenylalanine content of 1800 pmoles per A_{260} unit.

† From the Departments of Biochemistry and Medical Genetics, University of Oregon Medical School, Portland, Oregon. *Received December 6, 1971.* Supported by Grant GM-16299 from the National Science Foundation and Grant CA-13173 from the National Institutes of Health.

* Career Development awardee of the National Institute of General Medical Sciences.

‡ Fellow in Medical Genetics supported by NIH Training Grant HD-00165.

[1] Abbreviations used are: Phe-tRNA synthetase, phenylalanyl-tRNA synthetase; BD-cellulose, benzoylated DEAE-cellulose; G*, the kethoxal adduct of guanosine; A*, 2-thiomethyl-6-isopentenyladenosine.

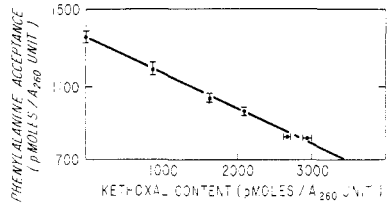

FIGURE 1: Effect of kethoxalation on phenylalanine acceptance of yeast $tRNA^{Phe}$. The dimensions of the points reflect the range of values obtained in duplicate determinations.

Aminoacyl-tRNA Synthetases. A crude preparation of *E. coli* aminoacyl-tRNA synthetases was obtained according to the method of von Ehrenstein (1967). Crude preparations of yeast aminoacyl-tRNA synthetases were obtained by a similar procedure, except that frozen Baker's yeast was used as a source. The cells were broken by grinding with glass beads in a Virtis homogenizer and the preparations were stored at −20° as suspensions in 90% saturated $(NH_4)_2SO_4$ containing 10 mM dithiothreitol. Just before use, portions of the suspension were centrifuged, the pellets were dissolved in 50 mM Tris-Cl^- (pH 7.3) and the solutions were freed of $(NH_4)_2SO_4$ by passage through small Sephadex G-25 columns equilibrated with the same buffer.

Assays of Amino Acid Acceptance. Assays for phenylalanine acceptance of untreated and kethoxal-treated yeast $tRNA^{Phe}$ were performed according to Wimmer *et al.* (1968) except that the temperature of incubation was decreased to 0° to prevent loss of kethoxal from the tRNA during the assay. Kinetic studies of the aminoacylation of untreated and kethoxalated tRNA showed that in all cases, charging had reached a steady state within 30 min. This steady state was maintained for at least a further 30 min, indicating that nuclease activity was negligible under our assay conditions. It should also be pointed out that the yeast $tRNA^{Phe}$ used had essentially 100% of its terminal adenosine intact because of the method used for its isolation (Litt,1968).

Assays for phenylalanine acceptance of *E. coli* $tRNA^{Phe}$ and $tRNA_1^{Val}$ catalyzed by yeast Phe-tRNA synthetase were performed as described by Dudock *et al.* (1970, 1971) except that crude synthetase preparations were used. Assays for valine acceptance of *E. coli* $tRNA_1^{Val}$ and for phenylalanine acceptance of *E. coli* $tRNA^{Phe}$ catalyzed by *E. coli* synthetases were performed as described by Kelmers *et al.* (1965) and Dudock *et al.* (1971), respectively.

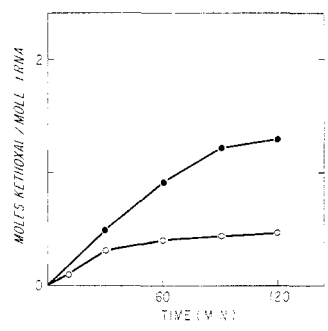

FIGURE 2: Kinetics of reaction of [^{3}H]kethoxal with *E. coli* $tRNA_1^{Val}$ and *E. coli* $tRNA^{Phe}$. Reaction mixtures contained, per milliliter of final volume, 35 A_{260} units of tRNA, 100 μmoles of sodium cacodylate (pH 7.0), 10 μmoles of $MgCl_2$, and 15 μmoles of ^{3}H-labeled kethoxal. Each point represents the average of two determinations. Solid circles, $tRNA_1^{Val}$; open circles, $tRNA^{Phe}$.

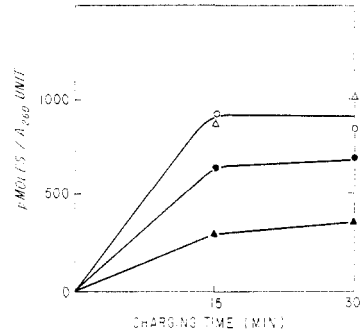

FIGURE 3: Effect of kethoxalation on the charging of *E. coli* $tRNA_1^{Val}$ with valine and phenylalanine. Aminoacylation with phenylalanine was performed at 30° in a total volume of 0.10 ml containing: 50 mM potassium cacodylate (pH 5.8)–0.4 mM EDTA–2.5 mM ATP–20 mM $MgCl_2$–0.05 mM [^{14}C]phenylalanine (10 Ci/mole)–0.14 A_{260} unit of $tRNA_1^{Val}$, and a saturating amount of crude yeast synthetase prepared as described in the text. Aminoacylation with valine was performed as described by Kelmers *et al.* (1965). Open circles, untreated tRNA and valine; closed circles, untreated tRNA and phenylalanine; open triangles, kethoxalated tRNA and valine; closed triangles, kethoxalated tRNA and phenylalanine.

Structural Characterization of Kethoxalated tRNAs. Digestion of tRNAs with phenol-extracted T_1 RNase and chromatography on DEAE-cellulose in 7 M urea were performed as previously described (Litt, 1971) except that the columns were packed under a pressure of about 15-cm mercury according to the method of Powers (1970) and urea was purified by the method of Birnboim and Glickman (1969).

Concentration and desalting of oligonucleotides was accomplished according to the method of Birnboim and Glickman (1969) with several modifications. Initially, the column fractions were diluted with water to a urea concentration less than 5 M (H. C. Birnboim, 1971, personal communication). To free the oligonucleotides of oxalic acid, the solutions were brought to a pH of 8–9 with NH_4OH and then passed through columns of Bio-Gel P-2 (Uziel, 1967). Nucleoside compositions were determined by the method of Randerath and Randerath (1971).

Reaction of [^{3}H]Kethoxal with tRNA. Kinetic studies of the reaction of [^{3}H]kethoxal with various tRNAs were performed at 25° as previously described (Litt, 1971) except that acid-precipitable radioactivity was determined by the method of Birnboim (1970). Preparative kethoxalation of all the tRNAs used in this study was performed for 2 hr at 25° in 0.1 M sodium cacodylate (pH 7.0), 10 mM $MgCl_2$, and 15 mM [^{3}H]kethoxal (4 Ci/mole). These were the conditions used previously to label G's at positions 20 and 34 in yeast $tRNA^{Phe}$ (Litt, 1971).

Results

Inactivation of Yeast $tRNA^{Phe}$. Figure 1 shows that there is a good linear correlation between the degree of kethoxalation and the degree of inactivation of yeast $tRNA^{Phe}$. This linearity, with no evidence for a lag at low extents of kethoxalation, rules out multiple-hit mechanisms for inactivation.

Inactivation of (E. coli) $tRNA_1^{Val}$ and $tRNA^{Phe}$. Figure 2 shows the time course of the reaction of (*E. coli*) $tRNA_1^{Val}$ with kethoxal. After 2 hr, approximately 1.3 moles of kethoxal have reacted per mole of tRNA. Figure 3 shows the results of acceptor assays of untreated and 2-hr kethoxalated $tRNA_1^{Val}$ using a homologous synthetase preparation with valine and a heterologous synthetase preparation with phenylala-

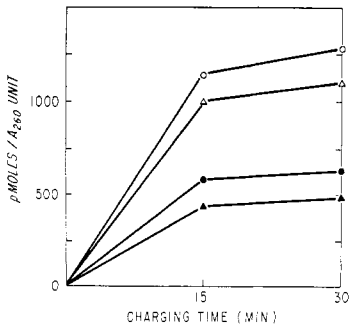

FIGURE 4: Effect of kethoxalation on the charging of *E. coli* $tRNA^{Phe}$ with yeast and *E. coli* synthetase. Aminoacylation with phenylalanine was performed in a total volume of 0.10 ml containing: 50 mM Tris (pH 7.6)–0.5 mM EDTA–20 mM $MgCl_2$–2.5 mM ATP–0.05 mM [^{14}C]phenylalanine (10 Ci/mole)–0.1–0.2 A_{260} unit of $tRNA^{Phe}$, and a saturating amount of crude yeast or *E. coli* synthetase prepared as described in the text. Open circles, untreated tRNA and *E. coli* synthetases; closed circles, kethoxalated tRNA and *E. coli* synthetases; open triangles, untreated tRNA and yeast synthetases; closed triangles, kethoxalated tRNA and yeast synthetases.

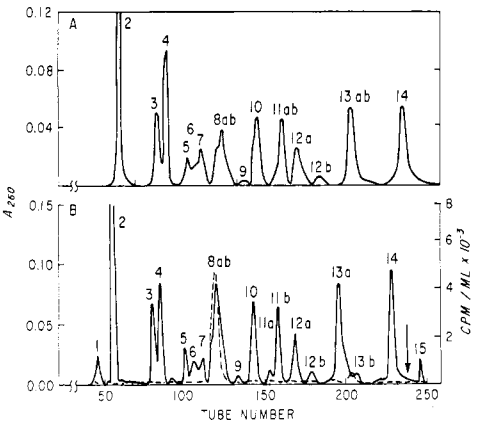

FIGURE 5: Elution profiles of 13 A_{260} units of T_1 RNase digests of untreated (A) and kethoxalated (B) *E. coli* $tRNA_1^{Val}$. Solid line, A_{260}; dashed line, radioactivity of ^{3}H from the [^{3}H]kethoxal used. At the point shown by the arrow the columns were stripped with 0.5 M NaCl in starting buffer.

nine. It is clear that kethoxalation has no effect on the homologous reaction but causes an approximately 50% decrease in the extent of "mischarging" in the heterologous reaction.

Figure 2 also shows the time course of the reaction of *E. coli* $tRNA^{Phe}$ and kethoxal. After 2 hr, approximately 0.5 mole of kethoxal has reacted per mole of tRNA. Figure 4 shows the results of acceptor assays of untreated and kethoxalated *E. coli* $tRNA^{Phe}$ using homologous and heterologous synthetases. In contrast to the case of $tRNA_1^{Val}$, kethoxalation of *E. coli* $tRNA^{Phe}$ inhibits the homologous and heterologous reactions to equal extents.

It is of interest that under reaction conditions that allow the labeling of two residues in yeast $tRNA^{Phe}$ and approximately one residue in *E. coli* $tRNA_1^{Val}$, only 0.5–0.6 residue of *E. coli* $tRNA^{Phe}$ become labeled. As the target site in *E.* coli $tRNA^{Phe}$ is G-34 (see below) this suggests that our *E. coli* $tRNA^{Phe}$ preparation is heterogeneous with respect to the modification of G-34 or the availability of G-34 for reaction.

As aggregation might reduce the availability of G-34, we studied the effect of preheating on the kinetics of kethoxalation of *E. coli* $tRNA^{Phe}$. A tRNA sample, dissolved in 0.1 M sodium cacodylate–0.01 M $MgCl_2$ (pH 7.0), was heated for 1 min at 80°, a treatment which breaks up aggregates in yeast $tRNA^{Ser}$ (Zachau, 1968). After cooling to 25°, [^{3}H]-kethoxal was added and the kinetics of kethoxalation were followed. The results obtained were identical with those obtained without preheating. For this reason, we suspect that the low reactivity of G-34 in (*E. coli*) $tRNA^{Phe}$ is not due to aggregation but is due to a partial chemical modification of G-34 or to the existence of part of the $tRNA^{Phe}$ in a conformation in which G-34 is unavailable.

Location of Kethoxalated Residues. E. coli $tRNA_1^{Val}$. T_1 RNase profiles of untreated and kethoxalated $tRNA_1^{Val}$ are shown in Figure 5. A major radioactive peak, accounting for about 50% of the tritium recovered from the column, was eluted just prior to uv peak 8. The remaining 50% of the radioactivity was distributed broadly over the elution profile with a minor peak at tube 202. Comparison of our elution profiles with those of Harada *et al.* (1971) suggests that uv peak 8 contains the tetranucleotide TpψpCpGp. This in turn suggests, but does not prove, that the major radioactive peak is G*pApGp, the same kethoxalated oligonucleotide found to elute just prior to TpψpCpGp in T_1 RNase digests of kethoxalated yeast $tRNA^{Phe}$ (Litt, 1969). An oligonucleotide of this structure would arise from T_1 RNase digestion of a GpG*pApGp sequence. Evidence supporting this hypothesis comes from comparison of the areas under the uv peaks of the T_1 RNase profiles of untreated and kethoxalated $tRNA_1^{Val}$ (Table I). These data show that kethoxalation causes a significant decrease in the amount of peak 4 (ApGp) together with a significant increase in the area under peak 8. The only other part of the elution profile which changed significantly was peak 13 A + B. The reason for the increase in uv-absorbing material under this peak is not clear, but might be due to contribution from a kethoxalated oligonucleotide comprising the minor radioactive peak at fraction 202.

The data presented so far are also compatible with the assignment of structure ApG*pGp to the radioactive oligonucleotide in peak 8 of Figure 5. Such an oligonucleotide

TABLE I: Relative Areas under Peaks in Elution Profiles of T_1 RNase Digests of Untreated and Kethoxalated *E. coli* $tRNA_1^{Val}$.

Peak	Area Relative to Peak 10	
	Untreated	Kethoxalated
2	2.3	2.1, 1.9
3	0.93	0.94, 1.1
4	1.31	1.10, 1.04
5, 6, 7[a]	1.11	1.09, 1.20
8	1.32	1.65, 1.84
10	1.00	1.00, 1.00
11 A + B[a]	1.09	1.02, 1.06
12A	0.68	0.69, 0.78
13 A + B[a]	1.67	2.1, 2.1
15	1.76	1.61, 1.74

[a] These peaks were not always completely resolved and hence were combined for the purpose of measuring their areas by planimetry.

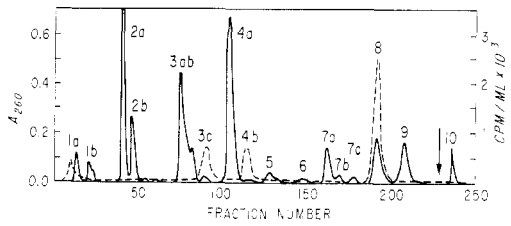

FIGURE 6: Elution profile of pancreatic RNase digest of kethoxalated *E. coli* $tRNA_1^{Val}$. 17 A_{260} units of kethoxalated $tRNA_1^{Val}$ were digested with 50 μg of pancreatic RNase A in 0.20 ml of 50 mM $Na_2B_4O_7$–8 mM EDTA (pH 7.7) for 2 hr at 37°. The digest was chromatographed on DEAE-cellulose as described in Methods. At the point shown by the arrow the column was stripped with 0.6 M NaCl in starting buffer. Solid line, A_{260}; dashed line, radioactivity of ^3H from the [^3H]kethoxal used.

would arise from T_1 RNase digestion of a GpApG*pGp sequence.

In order to rule out one of these alternatives, we digested a sample of kethoxated (*E. coli*) $tRNA_1^{Val}$ with pancreatic RNase and chromatographed the digest on DEAE-cellulose. The elution profile (Figure 6) showed a major radioactive peak coeluting with uv peak 8 which accounted for 50% of the radioactivity recovered from the column. Comparison of this elution profile with that of Figure 8 of Harada *et al.* (1971) allows us to assign the structure GpGpGpApGpApGpCp to our uv peak 8. This oligonucleotide contains a GpGpApGp sequence but lacks a GpApGpGp sequence. From this we conclude that the major site of kethoxalation in *E. coli* $tRNA_1^{Val}$ is at the third residue from the 5′ end of this pancreatic RNase octanucleotide. Inspection of the published sequence for *E. coli* $tRNA_1^{Val}$ (Yaniv and Barrell, 1969; Kimura *et al.*, 1971) shows that this corresponds to position 20 of the tRNA chain.

The minor radioactive peaks 3c and 4b of Figure 6, which accounted for about 20% of the radioactivity recovered from the column, were not investigated further. These peaks may have arisen through nonspecific cleavages of pancreatic RNase on peak 8.

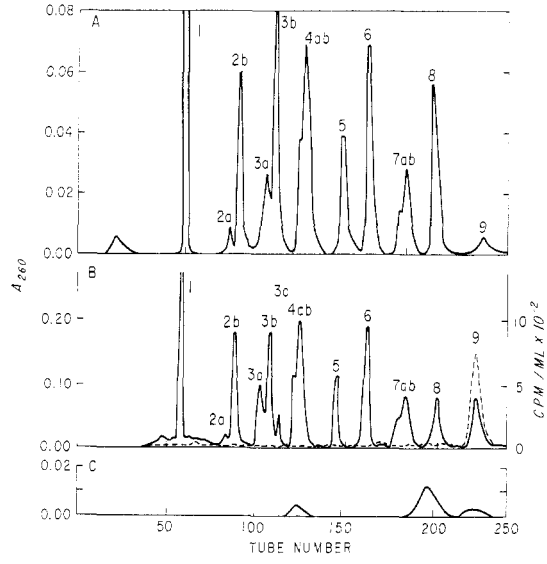

FIGURE 7: Elution profiles of T_1 RNase digests of 4.5 A_{260} units of untreated (A) and 14 A_{260} units of kethoxalated (B) *E. coli* $tRNA^{Phe}$ and of 0.60 A_{260} unit of peak 9 from a digest of kethoxalated $tRNA^{Phe}$ after removal of kethoxal and redigestion with T_1 RNase (C). Solid line, A_{260}; dashed line, radioactivity of ^3H from the [^3H]kethoxal used.

TABLE II: Analysis of Peak 8 from Untreated *E. coli* $tRNA^{Phe}$.

Nucleoside	Mole Fraction: Observed	Mole Fraction: Predicted for $C_4A_3A^*\psi G$
G	0.107	0.111
C	0.474	0.444
A	0.290	0.333
ψ	0.129	0.111
A*	*a*	0.111

[a] A* would be expected to travel with the solvent front in chromatographic systems F and G of Randerath and Randerath (1971) and would therefore not have been detected in this work.

E. coli $tRNA^{Phe}$. T_1 RNase profiles of untreated and kethoxalated *E. coli* $tRNA^{Phe}$ are shown in Figure 7A,B. The kethoxalated material has a single major radioactive peak coeluting with uv peak number 9. From inspection of the uv profiles of Figure 7A,B, it is apparent that kethoxalation causes a decrease in the area under peak 8 and a corresponding increase in the area under peak 9.

As peak 8 is the latest eluting major peak in control T_1 digests, we assume that it corresponds to the decanucleotide found by Barrell and Sanger (1969) to be the largest oligonucleotide in T_1 digests of this tRNA. This assumption was validated by nucleoside analysis of peak 8 from Figure 7A (Table II).

Kethoxal was removed from peak 9 of Figure 7B by desalting the peak on a small DEAE-cellulose column (Litt, 1969). After redigestion with T_1 RNase, the material was rechromatographed under conditions identical with those used for the columns of Figure 7A,B. The results (Figure 7C) show that peak 9 of Figure 7B contains oligonucleotides which appear in peaks 4a,b and 8 of complete T_1 RNase digests of untreated tRNA.

From the data presented above and from the published sequence of *E. coli* $tRNA^{Phe}$ (Barrell and Sanger, 1969), we conclude that the ^3H-labeled oligonucleotide in peak 9 of Figure 7B is ApψpUpG*pApApA*pApψpCpCpCpCpGp and that the primary site of kethoxalation is at site 34, the 5′-terminal nucleotide of the anticodon.

Discussion

Proof that kethoxal inactivation of yeast $tRNA^{Phe}$ is a single-hit process strongly supports our theory that the stereoisomerism of the kethoxal adduct formed at the target site determines whether or not derivatization leads to inactivation (Litt, 1971). The stoichiometry of inactivation is also consistent with our theory. Thus, we observe only 35% inactivation when 1 mole of kethoxal has reacted per mole of tRNA (Figure 1). Presumably only 35% of the kethoxal molecules which have reacted at this point have formed adducts which are oriented appropriately to inactivate the tRNA. Unfortunately, the data at hand do not yet allow us to identify which site, G-20 or G-34, is the target or to eliminate the possibility that either site can act as a target for inactiva-

tion. Indeed, the data on inactivation of *E. coli* tRNAs reported in this paper make this latter possibility seem quite likely.

Figure 8 shows cloverleaf models for the three tRNAs we have studied. The arrows show the primary sites of kethoxalation. All of these tRNAs can be aminoacylated with phenylalanine by (yeast) Phe-tRNA synthetase and this aminoacylation is partially inhibited by kethoxalation.

Dudock *et al.* (1970, 1971) have proposed that the recognition site for yeast Phe-tRNA synthetase is contained in the stem of the dihydrouridine loop. Our results with $tRNA_1^{Val}$ tend to support this proposal because G-20, the target site for inactivation, lies close to the putative recognition site.

The fact that kethoxal inactivation of chargeability of $tRNA_1^{Val}$ by yeast Phe-tRNA synthetase is only 50% complete can be explained if, as in the case of yeast $tRNA^{Phe}$, proper orientation of the α-ethoxyethyl group of the kethoxal adduct were essential for inactivation.

The Dudock model does not predict our observation that kethoxalation of the anticodon G at position 34 in *E. coli* $tRNA^{Phe}$ inactivates the chargeability of this molecule with yeast Phe-tRNA synthetase. Position 34 cannot be part of the specific recognition site for yeast Phe-tRNA synthetase as there is no G at this position in *E. coli* $tRNA_1^{Val}$. Perhaps kethoxalation at this site, by introducing a bulky group, interferes sterically with a nonspecific interaction between tRNA and synthetase which is essential for charging to occur. A further possibility is that kethoxalation of the anticodon G perturbs the tertiary structure of the molecule in such a way as to cause inactivation.

The effects of kethoxalation of G-34 on the activity of *E. coli* and yeast $tRNA^{Phe}$ molecules are clearly different. In the case *E. coli* $tRNA^{Phe}$, there is a one-to-one correlation between kethoxalation and inactivation. In the case of yeast $tRNA^{Phe}$, kethoxalation at G-34 does not always lead to inactivation. We speculate that this difference may reflect a difference in the conformation of the anticodon loops of the two molecules. Although the anticodon loop of *E. coli* $tRNA^{Phe}$ is shown in Figure 8 in the standard conformation, with seven unpaired bases, we suggest that an additional base pair may form between ψ-32 and A-38. This would decrease the size of the anticodon loop to five bases and would cause its conformation to differ considerably from that of a seven-membered loop. As pointed out by Zachau and coworkers, a similar five-membered anticodon loop may also be present in (yeast) $tRNA^{Ser}$ (Zachau *et al.*, 1966).

Befort *et al.* (1970) present data showing that complexing of yeast $tRNA^{Phe}$ with purified yeast Phe-tRNA synthetase at pH 6.0 partially protects the tRNA against attack by T_1 RNase. Although they did not report which G sites are protected, their approach seems capable of yielding valuable information about the nature of tRNA–synthetase interactions. Unfortunately, G-34 of yeast $tRNA^{Phe}$ is 2′-O-methylated and hence resistant to T_1 RNase even in the free tRNA. Hence such studies with this tRNA cannot yield information about interaction of the anticodon with yeast Phe-tRNA synthetase. By studying the kethoxalation of yeast $tRNA^{Phe}$ while it is bound to yeast Phe-tRNA synthetase, it should be possible to determine to what extent the anticodon of this tRNA interacts with its cognate synthetase.

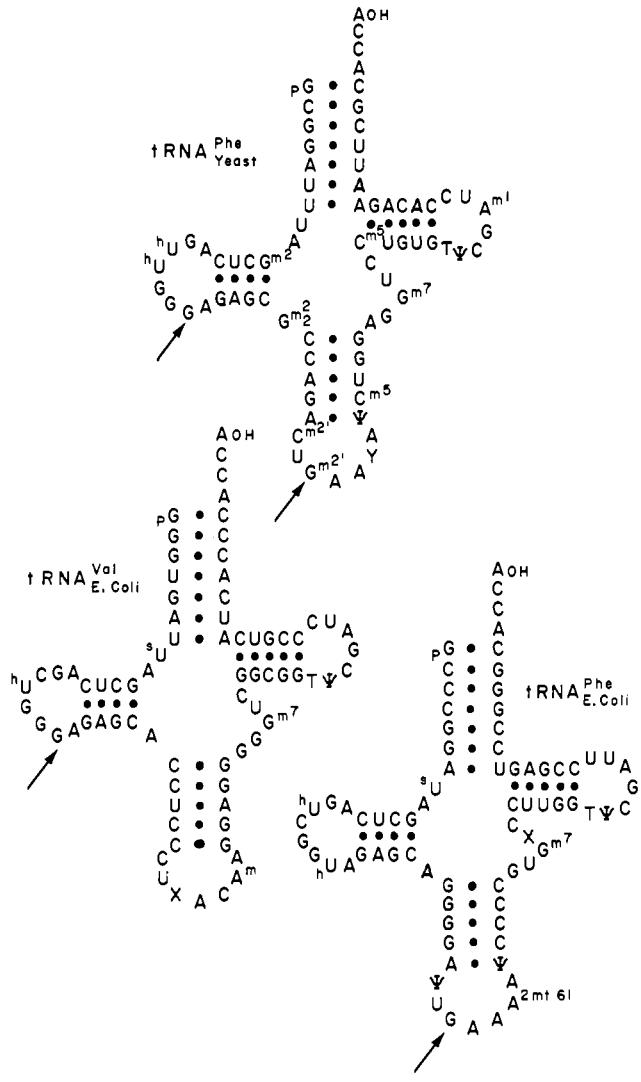

FIGURE 8: Primary structure of yeast $tRNA^{Phe}$ (RajBhandary and Chang, 1968), *E. coli* $tRNA_1^{Val}$ (Yaniv and Barrell, 1968), and *E. coli* $tRNA^{Phe}$ (Barrell and Sanger, 1969). The base $\times$ in *E. coli* $tRNA_1^{Val}$ is uridine-5-oxyacetic acid. Arrows mark the major sites of kethoxalation.

Acknowledgments

The authors thank Mr. Charles Lytle and Mr. Carroll Platz for excellent technical assistance, and are indebted to Dr. Robert W. Chambers for helpful discussion and constructive criticism.

References

Barrell, B. G., and Sanger, F. (1969), *FEBS (Fed. Eur. Biochem. Soc.) Lett. 3*, 275.

Befort, N., Fasiolo, F., Bollack, C., and Ebel, J. P. (1970), *Biochim. Biophys. Acta 217*, 319.

Birnboim, H. C. (1970), *Anal. Biochem. 37*, 178.

Birnboim, H. C., and Glickman, J. (1969), *J. Chromatogr. 44*, 581.

Dudock, B. S., DiPeri, C., and Michael, M. S. (1970), *J. Biol. Chem. 245*, 2465.

Dudock, B., DiPeri, C., Scileppi, K., and Reszelbach, R. (1971), *Proc. Nat. Acad. Sci. U. S. 68*, 681.

Gillam, I., Blew, D., Warrington, R. C., von Tigerstrom, M., and Tener, G. M. (1968), *Biochemistry 10*, 3459.

Harada, F., Kimura, F., and Nishimura, S. (1971), *Biochemistry 10*, 3269.

Kelmers, A. D., Novelli, G. D., and Stulberg, M. P. (1965), *J. Biol. Chem. 240*, 3979.

Kimura, F., Harada, F., and Nishimura, S. (1971), *Biochemistry 10*, 3277.
Litt, M. (1968), *Biochem. Biophys. Res. Commun. 32*, 507.
Litt, M. (1969), *Biochemistry 8*, 3249.
Litt, M. (1971), *Biochemistry 10*, 2223.
Powers, D. M. (1970), Ph.D. Thesis, Cornell University, p 60.
RajBhandary, U. L., and Chang, S. H. (1968), *J. Biol. Chem. 243*, 598.
Randerath, K., and Randerath, E. (1971), *in* Procedures in Nucleic Acid Research, Cantoni 'G. L., and Davies, D. R., Ed., Vol. 2, New York, N. Y., p 796.
Uziel, M. (1967), *Methods Enzymol. 12A*, 407.
von Ehrenstein, G. (1967), *Methods Enzymol. 12A*, 588.
Wimmer, E., Maxwell, I. H., and Tener, G. M. (1968), *Biochemistry 7*, 2623.
Yaniv, M., and Barrell, B. G. (1969), *Nature (London) 222*, 278.
Zachau, H. G. (1968), *Eur. J. Biochem. 5*, 559.
Zachau, H. G., Dutting, D., Feldman, H., Melchers, F., and Karau, W. (1966), *Cold Spring Harbor Symp. Quant. Biol. 31*, 417.

Isolation of Nuclei and Characterization of Ribonucleic Acid Synthesized *in Vitro* from Swine Aortic Tissue†

K. Janakidevi

ABSTRACT: The object of the present study was to devise a method for isolating substantial quantites of purified nuclei from aortic tissue, and to study the nature of the ribonucleic acids synthesized *in vitro* by the nuclei. A new method of homogenization is described using a stepwise disintegration of the tissue with a Virtis 60 homogenizer. This method gives a good yield of highly purified, enzymatically active nuclei. DNA-dependent RNA polymerase was assayed using the isolated nuclei and the product analyzed by nearest-neighbor base frequency analysis. At low ionic strength and in the presence of Mg^{2+}, the nuclei synthesize a ribosomal type of RNA while in the presence of Mn^{2+} and 0.3 M ammonium sulfate, a DNA-like RNA is produced. Some properties of the two reactions are also described.

Weiss (1960) first demonstrated the presence of DNA-dependent RNA polymerase (nucleoside triphosphate:RNA nucleotidyl transferase, EC 2.7.7.6) in an extract of nucleated cells, called the "aggregate enzyme." The existence of more than one polymerase was suggested by Widnell and Tata (1966) in rat liver nuclei, one active at low ionic strength in the presence of Mg^{2+}, and the other requiring high salt concentrations and Mn^{2+}. Solubilization and purification of RNA polymerases has since been reported, and it is generally agreed that there are at least two distinct enzymes in the nuclei of most eukaryote tissues examined, and a third one in some tissues (Roeder and Rutter, 1969, 1970). Intact nuclei provide a good system to study the nature of the RNAs synthesized during cell transformations.

The importance of DNA-dependent RNA synthesis in the developing and proliferating tissue has been well recognized. The formation of new nuclear mRNAs has been demonstrated in the early period of liver regeneration following partial hepatectomy (Church and McCarthy, 1967). It is generally accepted that when a cell passes from interphase to mitosis, a process of derepression is set into operation resulting in the synthesis of some messengers, which will in turn code for enzymes and proteins necessary for DNA synthesis.

During the development of atherosclerosis, some smooth muscle cells (SMC)[1] of the aortic intima media (Scott *et al.*, 1969) undergo proliferation. In experimental models, such as swine fed hypercholesteremic diets, increased DNA synthesis and cell division have been demonstrated (Florentin and Nam, 1968; Thomas *et al.*, 1968). Any investigation of the factors involved in SMC proliferation of the aorta in the atherosclerotic process must take into consideration the role of transcription and other nuclear functions. It is, therefore essential to develop a method for the isolation of substantial amounts of aortic nuclei in an enzymatically pure state. The present paper describes such a method and some of the properties of the RNA polymerases and the products they synthesize *in vitro*.

Materials and Methods

Male Yorkshire swine weighing 7–10 kg were used. They were on an unrestricted diet (commercial pig chow) and water was provided *ad libitum*.

ATP, GTP, CTP, UTP, and actinomycin D were purchased from Sigma Chemical Co., St. Louis, Mo. DNase and RNase are from Worthington Chemical Co. [^{3}H]UTP was obtained from New England Nuclear Corp., Boston, Mass. [α-^{32}P]-Nucleoside triphosphates were purchased from Schwarz BioResearch, New York, N. Y.

† From the Department of Pathology, Albany Medical College, Albany, New York 12208. *Received November 1, 1971.* Supported by NIH Grants HE-7155 and HE-14177, Research Grant from Albany Medical College, and a grant from the Heart Association of Eastern New York, Inc.

[1] Abbreviations used are: SMC, smooth muscle cells; nnf, nearest-neighbor frequency; RNase, ribonuclease; DNase, deoxyribonuclease.